

## ENTROPY GENERATION AND HEAT TRANSFER FOR REACTIVE, MAGNETO-HYDRODYNAMIC FLOW OF A JEFFREY FLUID OVER A STRETCHING SHEET

Jacob A. Gbadeyan and Joseph O. Akinremi

Department of Mathematics, Faculty of Physical Sciences, University of Ilorin, Ilorin, Nigeria.

### Abstract

---

*This study investigates entropy generation for the steady two-dimensional laminar forced convection and heat transfer of reactive, magneto-hydrodynamic flow of an incompressible Jeffrey fluid over a linearly stretching, impermeable and isothermal sheet. The governing differential equations of the model were transformed using appropriate similarity transformation to two nonlinear coupled ordinary differential equations (ODEs). The ODEs are solved numerically by shooting technique coupled with fourth order Runge-Kutta method using MAPLE 18. The results obtained from momentum and energy equations were used to compute the entropy generation rate and the irreversibility ratio. The influence of various emerging governing parameters of the flow and heat transfer such as Deborah number, ratio of relaxation to retardation times, Prandtl number, Eckert number, Reynolds number, Brinkmann number, Frank-kamentski parameter, activation energy parameter and magnetic term on dimensionless velocity, temperature, entropy generation and Bejan ratio were analyzed. A comparative analysis of the present numerical results with an exact solution for the dimensionless velocity  $f''(0)$  at the sheet surface is also carried out and it is observed that these two solutions are in excellent agreement.*

---

**Keywords:** Heat and Mass transfer, Reactiveness, Jeffrey fluid, MHD, Entropy Generation.

### 1. Introduction

Recent works have reflected so much interest by researchers in the flows of non-Newtonian fluids. This is due to wide range of its applications in chemical industries, petroleum industries, geophysics and biological fields. The flow of non-Newtonian fluids are governed by equations that are naturally more complex than the Navier-Stokes equations. The governing equations for the flows of non-Newtonian fluids are the reason for the constitutive relations which are used to predict the rheological behaviour of these fluids. Many constitutive relations have been considered in literatures due to versatile nature of non-Newtonian fluids; one of which is the Jeffrey fluid, which differs from the other models is the fact that it is a linear model which uses time derivatives to measure the relaxation to retardation times. However, the simplest type of non-Newtonian fluids is the Maxwell fluid model which uses convected derivatives. Moreover, the study of fluid flow over a stretching sheet has gained considerable attention due to regular occurrences in many industries and manufacturing processes, such as; polymer sheet or filament production, drawing of plastic films and so on. Sakiadis[1] was the first to study the boundary layer flow over stretching surface with a constant velocity and formulated boundary layer equation for two-dimensional asymmetric flows. Later, the work was extended by Crane[2], who investigated the problem of a stretching sheet whose velocity is proportional to the distance from the slit. Since then, many studies have been carried out taking into consideration the effects of stretching along with other various physical effects.

Molla and Yao [3] investigated mixed convection heat transfer of non-Newtonian fluids over a flat plate using a modified power law viscosity model. Hence, they solved the boundary layer equations using finite difference method and presented the numerical results for the shear-thinning fluid with respect to velocity and temperature distribution. Hayat *et al.*, [4] investigated the magneto-hydrodynamic(MHD) flow of a Jeffrey fluid in a channel. They constructed series solution to the non-linear problem with the use of homotopy analysis method(HAM). Prasad *et al.*, [5] studied the steady viscous incompressible two-dimensional MHD flow of an electrically conducting power law fluid over a vertically stretching sheet. They assumed the stretching of the surface and the prescribed surface temperature to vary linearly with the distance from the slit and solved the boundary layer equations using Keller's box method.

---

Corresponding Author: Akinremi J.O., Email: akinremijoseph@gmail.com, Tel: +2348060612530

Hayat *et al.*, [6] investigated the unsteady boundary layer flow and heat transfer of an incompressible Jeffrey fluid over a linearly stretching sheet. They got the analytical solution of the system of differential equations using homotopy analysis technique. Qasim [7] studied the effects of heat and mass transfer in Jeffrey fluid over a stretching sheet in the presence of heat source/sink. He derived exact solution by power series method using Kummer's confluent hyper-geometric functions and examined the effects of the emerging parameters on velocity, temperature and concentration profiles. Idowu *et al.*, [8] examined the effects of heat transfer on unsteady MHD oscillatory flow of Jeffrey fluid in a horizontal channel with chemical reaction. The temperature prescribed at plates is uniform and asymmetric. A perturbation method was deployed to solve the momentum and energy equation. Nadeem *et al.*, [9] numerically studied the steady two-dimensional flow of a Jeffrey fluid over a linearly stretching sheet in the presence of nanoparticles. Idowu *et al.*, [10] studied the impact of heat and mass transfer on MHD oscillatory flow of Jeffrey fluid in a porous channel with thermal conductivity, dufour and sores. The partial differential equations governing the flow were solved numerically using semi-implicit finite difference scheme with the aid of MATLAB software, Jena *et al.*, [11] examined chemical reaction effects on MHD Jeffrey fluid over a stretching sheet through porous media with heat generation/absorption. Rundora [12] studied the laminar flow in a channel filled with saturated porous media and used fourth order Runge-Kutta method with shooting technique in solving the differential equations.

Entropy generation being the measure of the destruction of available work of the system, the determination of the active factors motivating the entropy generation is important in upgrading the system performances. Thus, several useful studies on entropy generation have been carried out by researchers. Bejan [13, 14, 15] gave analysis of the second law of thermodynamics inherent irreversibility in heat transfer with thermal design of an engineering system and entropy generation minimization. Butt [16] discussed the effects of velocity slip on entropy generation in the boundary layer flow over a vertical surface with convective boundary condition. They numerically solved the governing equations using shooting method and presented expressions for the entropy generation and Bejan number. Butt and Ali [17] studied the effects of entropy generation on MHD flow over a permeable stretching sheet embedded in a porous medium in the presence of viscous dissipation. Dehsara *et al.*, [18] investigated the entropy generation of MHD mixed convection flow over a nonlinear stretching, inclined and transparent plate embedded in a porous medium. Dalir [19] studied the entropy generation for the steady two-dimensional laminar convection flow and heat transfer of an incompressible Jeffrey non-Newtonian fluid over a linearly stretching, impermeable and isothermal sheet numerically. However, he didn't consider the effects of MHD and reactivity. The governing differential equations of continuity, momentum, and energy were transformed using suitable similarity transformations to the two nonlinear coupled ordinary differential equation (ODEs). The ODEs were solved using implicit Keller's box method, Adesanya *et al.*, [20] discussed the entropy generation analysis for reactive couple stress fluid flow through a channel saturated with porous materials and Gbadeyan *et al.*, [21] studied the effects of slippage and couple stresses in entropy generation in a porous channel filled with highly porous medium.

Uddin *et al.*, [22] investigated the steady two-dimensional laminar mixed convective boundary layer nanofluid flow in a Darcian porous medium due to a stretching/shrinking sheet with slip. The governing boundary-value problem transformed to dimensionless form through linear group of transformations which yielded system of coupled similarity differential equations. The transformed equations were solved numerically using the Runge-Kutta-Fehlberg fourth-fifth-order numerical quadrature method from MAPLE symbolic software. Das *et al.*, [23] studied the entropy analysis on MHD, pseudo-plastic nanofluid flow through a vertical porous channel with convective heating. Three different types of nanoparticles (namely: copper, aluminium oxide and titanium dioxide) are considered with pseudo-plastic carboxymethyl cellulose (CMC) – water is used as a base fluid. The governing equations were solved numerically by shooting techniques coupled with Runge-Kutta scheme. Gireesha, *et al.*, [24] investigated the problem of MHD boundary layer flow and heat transfer of an electrically conducting dusty fluid over an unsteady stretching surface through a non-Darcy porous medium. The flow in porous medium is described by employing the Darcy-Forchheimer based model. The pertinent time-dependent equations, governing the flow and heat transfer are reduced into a set of non-linear ODEs with the aid of suitable similarity transformations. The transformed equations are numerically integrated using fourth-fifth order Runge-Kutta-Fehlberg method. Mabood *et al.*, [25] constructed the mathematical model for determining the effects of variable viscosity and thermal conductivity on unsteady Jeffrey flow over a stretching sheet in the presence of magnetic fluid and heat generation. The governing partial differential equations are transformed into a set of nonlinear ODEs and then solved by using Runge-Kutta-Fehlberg method with shooting technique. The available literatures surveyed revealed that the entropy generation and ratio of irreversibility have not yet been investigated for the flow and heat transfer of a reactive, magneto-hydrodynamic Jeffrey non-Newtonian fluid over a stretching surface. In other words and to the best of the author's knowledge, the investigation of entropy generation and Bejan number for the reactive, magneto-hydrodynamic flow and heat transfer of a Jeffrey fluid over a stretching sheet is presented for the first time in this study. The partial differential equations describing the boundary layer flow and heat transfer are transformed using similarity transformation to a system of two nonlinear ordinary differential equations which are then solved numerically by using shooting technique coupled with Runge-Kutta scheme. Various

profiles of dimensionless velocity, temperature, entropy generation and Bejan number are plotted and the effects of various parameters such as Deborah number, ratios of relaxation to retardation times, Reynolds number, Brinkmann number, Frank-Kamenetskii number, activation number and different kinetics are analyzed.

**2. MATHEMATICAL FORMULATION**

Consider a reactive, magneto-hydrodynamic two dimensional laminar flow of a non-Newtonian fluid over a flat horizontal sheet. The non-Newtonian fluid is assumed to be incompressible viscous Jeffrey fluid and the sheet is also assumed to be linearly stretching, isothermal and impermeable. The viscous dissipation effect is also taken into consideration.

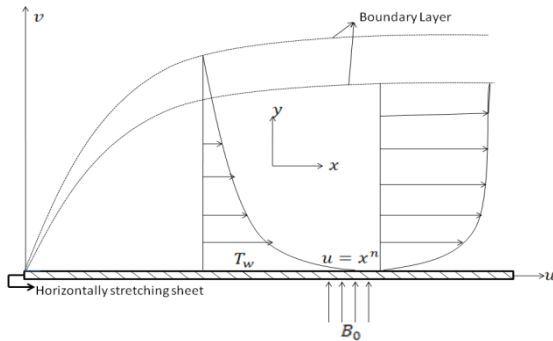


**Figure1: FLOW GEOMETRY**

The Jeffrey fluid model uses simple material derivatives which represent a rheology different from that of a Newtonian fluid. The Jeffrey model predicts relaxation/retardation time effects and the Cauchy stress tensor  $\tau$  for Jeffrey fluid is given as:

$$\tau = -pI + S \tag{1}$$

such that

$$S = \frac{\nu}{1+\xi} (\dot{\gamma} + \xi_1 \ddot{\gamma}) \tag{2}$$

where  $p$  is pressure,  $I$  is the identity and  $S$  is the extra stress tensor,  $\nu$  is dynamic/kinematic viscosity,  $\xi$  is the relaxation to retardation times,  $\xi_1$  is the relaxation time,  $\dot{\gamma}$  is the shear rate,  $\ddot{\gamma}$  is differentiated shear rate. The governing equations including mass, momentum and energy conservations are as follows[7 – 10]:

$$\frac{\partial u}{\partial x} + \frac{\partial v}{\partial y} = 0 \tag{3}$$

$$u \frac{\partial u}{\partial x} + v \frac{\partial u}{\partial y} = \frac{\nu}{(1+\xi)} \left\{ \frac{\partial^2 u}{\partial y^2} + \xi_1 \left( u \frac{\partial^3 u}{\partial x \partial y^2} - \frac{\partial u}{\partial x} \frac{\partial^2 u}{\partial y^2} + \frac{\partial u}{\partial y} \frac{\partial^2 u}{\partial x \partial y} + \nu \frac{\partial^3 u}{\partial y^3} \right) \right\} - \sigma_0 B_0^2 u \tag{4}$$

$$u \frac{\partial T}{\partial x} + v \frac{\partial T}{\partial y} = \alpha \frac{\partial^2 T}{\partial y^2} + \frac{\nu}{C_p(1+\xi)} \left\{ \left( \frac{\partial u}{\partial y} \right)^2 + \xi_1 \left( u \frac{\partial u}{\partial y} \frac{\partial^2 u}{\partial x \partial y} \right) + \left( \nu \frac{\partial u}{\partial y} \frac{\partial^2 u}{\partial y^2} \right) \right\} + \sigma_0 B_0^2 u^2 + Q C_0 A \left[ \frac{kT}{\nu l} \right]^m e^{-\frac{E}{RT}} \tag{5}$$

The boundary conditions are given as follows:

$$U = U_w(x) = ax, V = 0, T = T_w \text{ at } y = 0, \\ u \rightarrow 0, \frac{\partial u}{\partial y} \rightarrow 0, T \rightarrow T_\infty \text{ as } y \rightarrow \infty. \tag{6}$$

where  $T$  is the temperature variable,  $T_w$  is wall temperature,  $T_\infty$  is temperature of fluid far away from the sheet,  $Q$  is the heat of the reaction,  $E$  is the activation energy,  $C_p$  is the specific heat at constant pressure,  $k$  is the Boltzmann’s constant,  $A$  is the reaction rate,  $B_0^2$  is Uniform transverse magnetic field,  $\nu$  is Kinematic viscosity of the fluid,  $\sigma_0$  is the Stephan-Boltzmann constant,  $\alpha$  is thermal diffusivity of the fluid,  $R$  is the universal gas constant,  $C_0$  is the initial concentration, the sheet is stretched with velocity  $ax$ , where  $a$  is a real number,  $u$  and  $v$  are the velocity components in the  $x$  and  $y$  directions respectively. The following similarity transformations are used to transform the boundary layer flow and heat transfer equations to nonlinear ordinary differential equations(ODEs)

$$\eta = y \left( \frac{a}{b} \right)^{\frac{1}{2}}, f(\eta) = \frac{-\nu}{(av)^{\frac{1}{2}}}, f'(\eta) = \frac{u}{ax}, \theta(\eta) = \frac{E(T-T_0)}{RT_0^2}, \tag{7}$$

where  $\eta$ ,  $T_0$  and  $f$  are similarity variables and dimensionless stream function respectively.  $f'$  and  $\theta$  are the dimensionless velocity and temperature as well. The continuity equation is directly satisfied as:

$$u = \frac{\partial \psi}{\partial y}, v = -\frac{\partial \psi}{\partial x} \tag{8}$$

where  $\psi$  is the stream function. Thus,

$$\frac{\partial u}{\partial x} = af'(\eta), \frac{\partial u}{\partial y} = axf''(\eta), u \frac{\partial u}{\partial x} = a^2 x f'f''(\eta), \nu \frac{\partial u}{\partial y} = -a^2 x f f''(\eta) \tag{9}$$

From eq. (9) above, we can deduce:

$$\begin{aligned} \frac{\partial}{\partial y} &= \frac{\partial}{\partial \eta} \frac{\partial \eta}{\partial y} = \left(\frac{a}{v}\right)^{\frac{1}{2}} \frac{\partial}{\partial \eta} \\ \frac{\partial^2}{\partial y^2} &= \frac{\partial \eta}{\partial y} \left(\left[\frac{a}{v}\right]^{\frac{1}{2}} \frac{\partial}{\partial \eta}\right) = \left(\frac{a}{v}\right) \frac{\partial^2}{\partial \eta^2} \\ \frac{\partial^3}{\partial y^3} &= \frac{\partial \eta}{\partial y} \left(\left[\frac{a}{v}\right]^{\frac{1}{2}} \frac{\partial^2}{\partial \eta^2}\right) = \left(\frac{a}{v}\right)^{\frac{3}{2}} \frac{\partial^3}{\partial \eta^3} \\ \frac{\partial}{\partial x} &= \frac{\partial}{\partial \eta} \frac{\partial \eta}{\partial x} = 0 \end{aligned} \tag{10}$$

From the set of eq.(10), it can be established that  $\eta$  is not a function of  $x$ . Thus, using eq.(10), eq.(4) - eq.(6) are transformed to obtain the following:

$$f''' + (1 + \xi)(ff'' - f'^2) + \beta(f''^2 - ff^{iv}) - M^2 f' = 0 \tag{11}$$

$$\theta'' + Pr f \theta' + \frac{Pr \cdot Ec}{(1+\xi)} \left\{ f''^2 + \beta(f' f''^2 - f f'' f''') \right\} + M^2 f'^2 + \lambda(1 + \varepsilon \theta)^m e^{\frac{\theta}{(1+\varepsilon \theta)}} = 0 \tag{12}$$

and the boundary conditions are transformed as follows:

$$f(0) = 0, f'(0) = 1, \theta(0) = 1, f'(\infty) = 0, f''(\infty) = 0, \theta(\infty) = 0 \tag{13}$$

where

$$\beta = a \xi_1, M = \frac{\sigma_0 B_0^2 a^2}{v}, Pr = \frac{\mu C_p}{k}, Re = \frac{U_w x}{v}, Ec = \frac{(U_w)^2}{C_p R T_0^2} \tag{14}$$

Furthermore, the parameters that are of engineering interest are the local skin friction coefficient and the local Nusselt number, which are defined below as follows:

$$C_{f,x} = \frac{1+\beta}{1+\xi} \frac{f''(0)}{Re_x^{0.5}} \tag{15}$$

$$Nu_x = - \frac{\theta'(0)}{Re_x^{-0.5}} \tag{16}$$

### 2.1 ENTROPY GENERATION

The local entropy generation rate per unit volume for the Jeffrey fluid is as follows[10]:

$$S_{gen} = \frac{k}{T_0^2} \left(\frac{\partial T}{\partial y}\right)^2 + \frac{\mu}{T_0(1+\xi)} \left\{ \left(\frac{\partial u}{\partial y}\right)^2 + \xi_1 \left(u \frac{\partial u}{\partial y} \frac{\partial^2 u}{\partial x \partial y}\right) + \left(v \frac{\partial u}{\partial y} \frac{\partial^2 u}{\partial y^2}\right) + \sigma_0 B_0^2 u^2 \right\} \tag{17}$$

where the first term on the right hand side of eq.(17) is the entropy generation due to heat transfer and the second term is the entropy generation due to viscous dissipation and Jeffrey fluid effect. In order to define the dimensionless entropy generation number, a characteristic entropy generation rate  $(S_{gen})_0$  is defined as follows[10]:

$$(S_{gen})_0 = \frac{k}{T_0} \frac{\Delta T^2}{x^2} \tag{18}$$

Thus, the dimensionless entropy generation number is defined as the local ratio of volumetric entropy generation rate to the characteristic entropy generation rate:

$$N_s = \frac{S_{gen}}{(S_{gen})_0} \tag{19}$$

therefore, using the set of eq.(10); the dimensionless entropy generation rate for Jeffrey fluid flow is obtained as:

$$N_s = Re \cdot \theta'^2 + \frac{Br \cdot Re}{\Omega(1+\xi)} \cdot \{ f''^2 + \beta(f' f''^2 - f f'' f''') + M^2 f'^2 \} \tag{20}$$

where Re, Br and  $\Omega$  are the Reynolds number, the Brinkmann number and the dimensionless temperature difference respectively and are defined as:

$$Br = \frac{\mu \cdot (U_w)^2}{k \cdot \Delta T}, \Omega = \frac{\Delta T}{T_\infty} \tag{21}$$

In many engineering designs and optimization problems, the contribution of heat transfer entropy generation to total entropy generation rate is required; [35] presented an alternative irreversibility distribution parameter in terms of Bejan number (Be), which is defined[11]:

$$Be = \frac{N_1}{N_s} = \frac{1}{1+\phi} \tag{22}$$

where  $\phi = \frac{N_2}{N_1}$  is the irreversibility ratio. Entropy generation due to viscous dissipation dominates if  $\phi > 1$  and irreversibility due to heat transfer dominates if  $0 \leq \phi < 1$ , but when  $\phi = 1$ , it implies that both dominate equally. The Be takes the value between 0 and 1 [8].

### 3.0 METHOD OF SOLUTION AND VALIDATION OF RESULTS

The boundary-value problem comprising of eqns (11-13) were solved using efficient Runge-kutta method based on shooting technique with the aid of mathematical software(MAPLE 18). The detailed procedures of MAPLE are given in [31] and algorithm in Maple has been well tested for its accuracy, robustness and the effectiveness as established by [32], [33] and [34]. In order to validate and verify the accuracy of the applied numerical scheme, results of  $f''(0)$  for the following various values of  $\xi = 0.0, 0.2, \dots, 4.0$  and  $M = 0$  are shown in Table 1

below. The numerical values of dimensionless local skin friction group (lsfg),  $C_{f,x}Re_x^{0.5}$  for various parameters  $\beta$ ,  $\xi$ ,  $M$  using eq.(15) are depicted in **Table 2**. It is observed that  $C_{f,x}Re_x^{0.5}$  increases with an increase in  $\xi$  when  $\beta$  is held at a constant value. Thus, for an increase in the ratio of relaxation to retardation times  $\xi$  due to incrementation of relaxation duration of the non-Newtonian fluid, the velocity of the fluid near the sheet surface declines and the thickness of the hydrodynamic boundary layer increases, which in turn increases the local skin friction profile. Also, as Deborah number  $\beta$  increases, higher motion of the fluid particles inside the boundary layer is observed especially at the region of the sheet surface. Thus, the velocity of the boundary layer thickness lessens and results to lower skin friction coefficient value.

Furthermore, it is observed that as magnetic term  $M$  varied from 0 to 1.5, the  $C_{f,x}Re_x^{0.5}$  decreases for fixed values of  $\beta$  and  $\xi$ .

The influence of different physical parameters  $\xi$ ,  $\beta$ ,  $M$ ,  $Ec$ ,  $Pr$ ,  $\epsilon$ ,  $\lambda$ ,  $m$  on the dimensionless local Nusselt group  $-\theta'(0) = Nu_x Re_x^{-0.5}$  are presented in tabular form in **Table 3**. In the absence of magnetic term, (i.e.:  $M = 0$ ) and when Prandtl number is set at 1 (i.e.:  $Pr = 1$ ); it is observed that as Deborah number ( $\beta$ ) and activation energy parameter ( $\epsilon$ ) increase, the local Nusselt number group increases. While as each of ratio of relaxation to retardation times ( $\xi$ ), Eckert number ( $Ec$ ), Frank-Kamenetskii parameter ( $\lambda$ ) and chemical kinetics parameter ( $m$ ) increases the local Nusselt number group decreases. Although in the presence of magnetic term (i.e.:  $M = 1$ ) and Prandtl number is set to 1.3 (i.e.:  $Pr = 1.3$ ); it is noted that increase in ratio of relaxation to retardation times ( $\xi$ ) and activation energy parameter ( $m$ ) increases  $Nu_x Re_x^{-0.5}$ . While the local Nusselt number group  $Nu_x Re_x^{-0.5}$  reduces with an increase in each of the parameters: Deborah number ( $\beta$ ), Eckert number ( $Ec$ ), Frank-Kamenetskii parameter ( $\lambda$ ) and chemical kinetics parameter ( $m$ ).

**Table 1: Comparison of results for values of  $f''(0)$  and validation of present method(Runge-Kutta 4th order [RK4] based on shooting technique [ST]) with [10] using finite difference (FD) and [18] exact solution(eq. 11), for various values of  $\xi$ ; when  $\beta = 0.2$  and  $M = 0$ .**

$\xi$	$f''(0)$ Present Study	$f''(0)$ [10]	$f''(0)$ [18]
0.0	-0.91287094	-0.91468190	-0.91287093
0.2	-1.00000000	-1.00124052	-1.00000000
0.4	-1.08012345	-1.08100090	-1.08012345
0.6	-1.15470054	-1.15533663	-1.15470054
0.8	-1.22474487	-1.22521512	-1.22474487
1.0	-1.29099445	-1.29134772	-1.29099445
1.2	-1.35400640	-1.35427540	-1.35400640
1.4	-1.14471356	-1.41442077	-1.14471356
1.6	-1.47196014	-1.47212137	-1.47196014
1.8	-1.52752523	-1.52765178	-1.52752523
2.0	-1.58113883	-1.58123895	-1.58113883
2.2	-1.63299316	-1.63307294	-1.63299316
2.4	-1.68325082	-1.68331479	-1.68325082
2.6	-1.73205081	-1.73210240	-1.73205081
2.8	-1.77951304	-1.77955488	-1.77951304
3.0	-1.82574186	-1.82577595	-1.82574186
3.2	-1.87082869	-1.87085660	-1.87082869
3.4	-1.91485422	-1.91487716	-1.91485422
3.6	-1.95789002	-1.95790896	-1.95789002
3.8	-2.00000000	-2.00001569	-2.00000000
4.0	-2.04124145	-2.04125449	-2.04124145

**Table 2: Numerical values of local skin friction group  $C_{f,x}Re_x^{0.5}$  for various values of the physical parameters  $\beta$ ,  $\xi$ ,  $M$ .**

$\beta$	$\xi$	$C_{f,x}Re_x^{0.5}; M = 0$	$C_{f,x}Re_x^{0.5}; M = 1$	$C_{f,x}Re_x^{0.5}; M = 1.5$
0.1	0.0	-1.05072925	-1.48327617	-1.89076646
	0.6	-0.82955265	-1.05698303	-1.28619477
	1.2	-0.70722267	-0.85280720	-1.00566585
	1.8	-0.62682417	-0.73018218	-0.84175174
0.5	0.0	-1.22936117	-1.73215896	-2.20794115
	0.6	-0.96935755	-1.23432234	-1.50195284
	1.2	-0.82609376	-0.99588069	-1.17436528
	1.8	-0.73207367	-0.85267769	-0.98295466
2.0	0.0	-1.75360216	-2.44572106	-3.12203356
	0.6	-1.37551400	-1.74563268	-2.12394168
	1.2	-1.17024586	-1.40849024	-1.66075426
	1.8	-1.03629220	-1.20595605	-1.39008991

Furthermore, we also note that the presence of magnetic term (M) reduces the local Nusselt group  $Nu_x Re_x^{-0.5}$  for a fixed value of each of  $\xi, \beta$  in comparison with corresponding values of other parameters  $Ec, \varepsilon, \lambda, m$  when  $M = 0$ .

**Table 3:** Numerical values of local Nusselt number group  $Nu_x Re_x^{-0.5} = -\theta'(0)$  for various values of physical parameter.

M	Pr	$\xi$	$\beta$	$Nu_x Re_x^{-0.5}; Ec = 1$	$Nu_x Re_x^{-0.5}; Ec = 2$	$Nu_x Re_x^{-0.5}; Ec = 3$	$Nu_x Re_x^{-0.5}; \lambda = 0.1$	$Nu_x Re_x^{-0.5}; \lambda = 0.5$	$Nu_x Re_x^{-0.5}; \varepsilon = 3$	$Nu_x Re_x^{-0.5}; \varepsilon = 5$	$Nu_x Re_x^{-0.5}; m = -2$	$Nu_x Re_x^{-0.5}; m = 0$	$Nu_x Re_x^{-0.5}; m = 0.5$
0.0	1.0	0.0	0.1	-1.35928006	-1.78763095	-2.21615442	-0.48885494	2.58636832	-0.41765630	-0.22892055	-0.54344863	-3.65359120	-13.57900378
		0.6		-1.43462347	-1.79049707	-2.14646932	-0.57456707	2.73114759	-0.45962156	-0.25997359	-0.58439841	-4.39564439	-20.68808774
		1.2		-1.47349754	-1.78569615	-2.09795998	-0.62749734	2.79639502	-0.48376570	-0.27935029	-0.60532032	-4.89422448	-27.17311078
		1.8		-1.49354632	-1.77548429	-2.05746887	-0.66238918	2.82497131	-0.49850091	-0.29209901	-0.61639646	-5.24935961	-32.97536336
		0.0	0.5	-1.30453424	-1.78611541	-2.23795609	-0.43228751	2.46829145	-0.38859764	-0.20894637	-0.51266765	-3.19309858	-10.28882945
		0.6		-1.38654714	-1.78915617	-2.19190519	-0.51843412	2.64110859	-0.43245642	-0.23955917	-0.55841082	-3.90256533	-15.68445403
		1.2		-1.43579152	-1.79047141	-2.14524900	-0.57602233	2.73321754	-0.46030708	-0.26050522	-0.58502510	-4.40885405	
		1.8		-1.46618606	-1.78748334	-2.10885153	-0.61660807	2.78483655	-0.47894707	-0.27536235	-0.60136416	-4.78827382	
		0.0	1.0	-1.25491027	-1.78979536	-2.32504411	-0.38294157	2.34992269	-0.36257132	-0.19217574	-0.48355517	-2.80304760	-8.00983946
		0.6		-1.33683429	-1.78659520	-2.23656254	-0.46529204	2.53932900	-0.40566643	-0.22053066	-0.53096374	-3.45955464	-12.10423366
		1.2		-1.39164646	-1.78942903	-2.18734687	-0.52410882	2.65105438	-0.43526070	-0.24161171	-0.56118667	-3.95109925	-16.12524543
		1.8		-1.42915888	-1.79056508	-2.15207436	-0.56782533	2.71374966	-0.45643221	-0.25751071	-0.58146113	-4.33474926	
	1.3	0.0	0.1	-2.19294860	-3.01970669	-3.84682261	-1.06816762	3.32990730	-0.96397256	-0.76147660	-1.08480738	-5.24346703	-25.59518663
		0.6		-2.01926623	-2.62258749	-3.22608331	-0.99549114	3.27763461	-0.87602322	-0.67063277	-0.99370024	-5.53156217	-31.51099272
		1.2		-1.94330946	-2.43835759	-2.93351463	-0.96910307	3.25504152	-0.83162922	-0.62520338	-0.94590691	-5.76467369	-36.82647499
		1.8		-1.89879832	-2.32805400	-2.75738571	-0.95816129	3.23727566	-0.80284201	-0.59637129	-0.91384515	-5.94653202	-41.58295578
		0.0	0.5	-2.23520303	-3.16830743	-4.10393351	-1.07426491	3.29057470	-1.00473574	-0.80768135	-1.12782457	-4.82056239	-19.73441306
		0.6		-2.03987986	-2.72579111	-3.41076808	-0.98987097	3.24657990	-0.90801909	-0.70611937	-1.02956652	-5.11565718	-24.54148986
		1.2		-1.96097846	-2.52430136	-3.08778440	-0.96038859	3.23728161	-0.86071979	-0.65518193	-0.97996503	-5.37120754	-29.04066526
		1.8		-1.91704677	-2.40656493	-2.89619557	-0.94830547	3.23307768	-0.83099717	-0.62509741	-0.94772322	-5.58113399	-33.19872817
		0.0	1.0	-2.27442511	-3.31889359	-4.36409200	-1.08574444	3.24111796	-1.04532231	-0.85512532	-1.16869032	-5.19820740	-15.44902997
		0.6		-2.05960519	-2.82678750	-3.59433514	-0.98618413	3.19872778	-0.93837360	-0.74174061	-1.06183429	-4.97489589	-19.24085100
		1.2		-1.97208537	-2.60485008	-3.23784507	-0.95108649	3.19804024	-0.88716637	-0.68649818	-1.00952971	-4.71484071	-22.92244577
		1.8		-1.92630793	-2.47730792	-3.02846865	-0.93669017	3.20422702	-0.85583627	-0.65259232	-0.97658544	-4.43379474	-26.42685711

**4.0 GRAPHICAL ILLUSTRATION AND DISCUSSION OF RESULTS**

Entropy generation and heat transfer for reactive, magneto-hydrodynamic flow of a Jeffrey fluid over a stretching sheet have been investigated. Suitable similarity transformations are used to convert the governing equation to nonlinear ordinary differential equations(ODEs). Resultant nonlinear ODEs are then solved numerically.

**Fig. (2)** describes the dimensionless velocity profile  $f'(\eta)$  for various values of  $\xi$  when  $\beta = 0.2$  and  $M = 2$ . It is noticed that increase in  $\xi$  results in reduction of the boundary layer velocity of the fluid. This is expected, since the physical parameter  $\xi$  is inversely proportional to the retardation time of the non-Newtonian fluid. Thus, increase in  $\xi$  causes a decrease in fluid retardation time which prevents the fast track movement of the fluid motion, the thickness of the boundary layer diminishes and the velocity of the fluid is greatly augmented/aided.

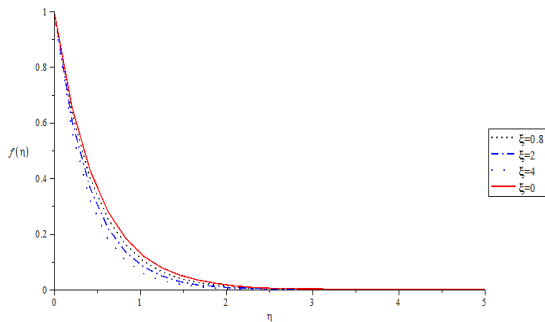


**Fig. 2:** Dimensionless velocity profiles  $f'(\eta)$  for various values of ratio of relaxation to retardation times  $\xi$ ; ( $\beta = 0.2, M = 2, Ec = 1.0, Pr = 0.71$ )

Thus, increase in  $\beta$  causes higher fluid motion in the boundary layer especially those adjacent to the surface sheet, one can then deduce that increase in Deborah number  $\beta$  consequently raises the fluid velocity.

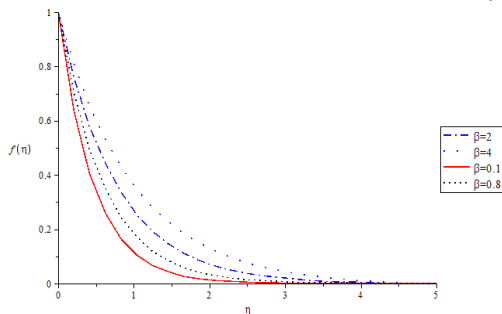


**Fig. 3:** Dimensionless velocity profiles  $f'(\eta)$  for various values of Deborah number  $\beta$ ; ( $\xi = 0.2, M = 2, Ec = 1.0, Pr = 0.71$ )

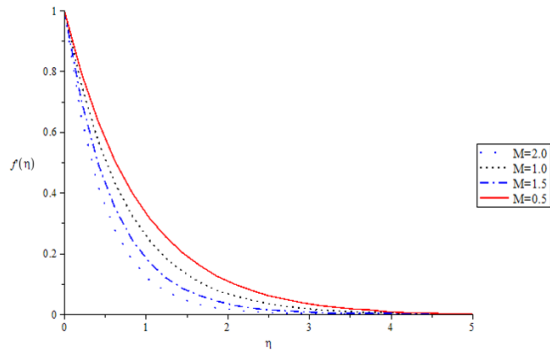


**Fig. 4:** Dimensionless velocity profiles  $f'(\eta)$  for various values of Magnetic parameter  $M$ ; ( $\xi, \beta = 0.2, Ec = 1.0, Pr = 0.71$ )

**Fig.(4)** depicts the dimensionless velocity profile  $f'(\eta)$  for various values of  $M$  when  $\beta = \xi = 0.2$ . It is noticed that the velocity's profile decreases as  $M$  increases and also observed that the momentum boundary layer thickness slightly decrease as  $M$  increases. This can be attributed to the presence of Lorentz force acting as a resistant to the flow and as a result the boundary layer becomes steeper.

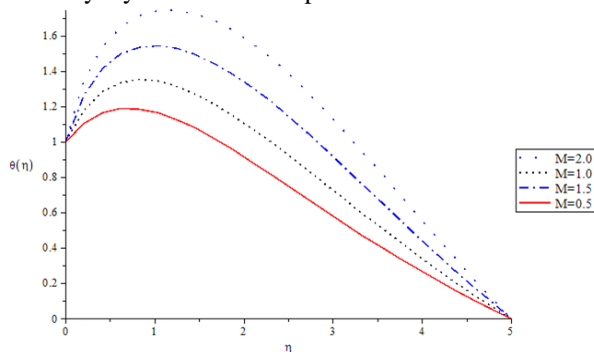


**Fig. 5:** Dimensionless temperature profiles  $\theta(\eta)$  for various values of Magnetic parameter  $M$ ; ( $\xi, \beta = 0.2, Ec = 1.0, Pr = 0.71, \varepsilon = 1, \lambda = 1, m = 0.5$ )

**Fig.(5)** illustrates the dimensionless temperature profile  $\theta(0)$  for various values of the Magnetic field  $M$ . It is observed that as  $M$  increases, the temperature profile increase. This can be associated with the presence of Lorentz force which enhances the flow's temperature. **Fig.(6)** reveals the dimensionless temperature profile  $\theta(0)$  for various values of ratio of relaxation to retardation time  $\xi$ . It is observed that  $\xi$  did not affect temperature much at the neighborhood of the sheet surface  $\eta = 0$ . Nevertheless, further into the boundary layer,  $\xi$  has a little noticeable effect in the temperature toward the other end ( $\eta = 1$ ), such that as  $\xi$  increases, the temperature slightly reduces. **Fig.(7)** reveals the effect of various values of Deborah number  $\beta$  on the dimensionless temperature profile  $\theta(0)$ . It is observed that  $\beta$  slightly boost the temperature in the sheet surface vicinity, such that  $\beta$  causes increase in temperature, but reverse is the case at the other end of the boundary layer. **Fig.(8)** displays the dimensionless temperature profile  $\theta(0)$  for various values of Prandtl number  $Pr$ . It is found that as  $Pr$  increases; the fluid temperature reduces and the reduction is more obvious at the sheet close to the boundary layer domain. this can be attributed to the fact that an increase in  $Pr$  is equivalent to a decrease in thermal diffusion of the fluid layer which results in a thin thermal boundary layer and hence lower temperature. **Fig.(9)** depicts the dimensionless temperature profile  $\theta(0)$  for various values of Eckert number  $Ec$ . It is seen that variation of  $Ec$  greatly influenced the temperature of the fluid inside the boundary layer. As a matter of fact, it is observed that  $Ec$  increases, so also the temperature. the  $Ec$  is proportional to the square of stretching velocity of the sheet.

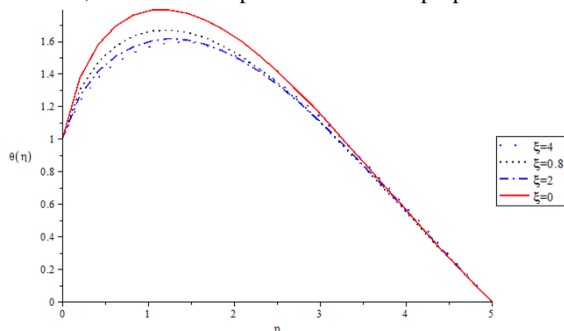


**Fig. 6:** Dimensionless temperature profiles  $\theta(\eta)$  for various values of ratio of relaxation to retardation times  $\xi$ ; ( $\beta = 0.2, M = 2, Ec = 1.0, Pr = 0.71, \varepsilon = 1, \lambda = 1, m = 0.5$ )

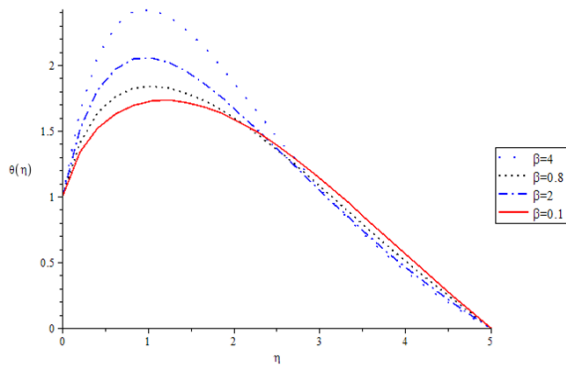


Fig. 7: Dimensionless temperature profiles  $\theta(\eta)$  for various values of Deborah number  $\beta$ ; ( $\xi = 0.2, M = 2, Ec = 1.0, Pr = 0.71, \varepsilon = 1, \lambda = 1, m = 0.5$ )

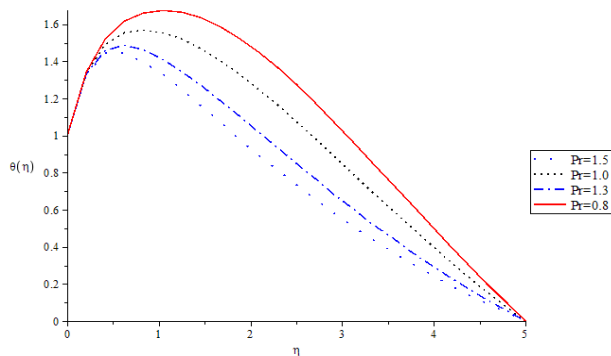


Fig. 8: Dimensionless temperature profiles  $\theta(\eta)$  for various values of Prandtl number  $Pr$ ; ( $\xi, \beta = 0.2, M = 2, Ec = 1.0, \varepsilon = 0.1, \lambda = 1, m = 0.5$ )

Fig.(10) displays the dimensionless temperature profile  $\theta(0)$  for various values of Frank-kameneskii parameter  $\lambda$ . It is observed that as  $\lambda$  increases, the temperature profile also increases inside the boundary layer. This is due to the rate of internal heat generation activities contributed by exothermic chemical reaction in the system while Fig.(11) displays the dimensionless temperature profile  $\theta(0)$  for various values of activation energy parameter  $\varepsilon$ . It is noticed that the fluid temperature decreases as the  $\varepsilon$  increases.

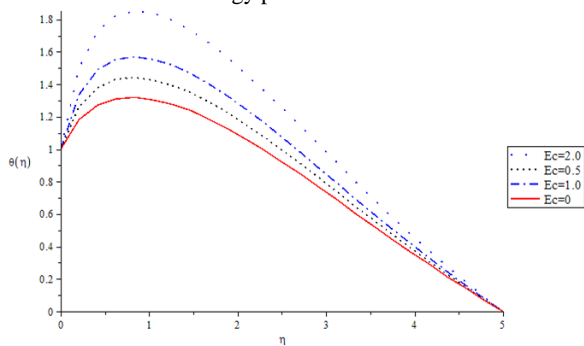


Fig. 9: Dimensionless temperature profiles  $\theta(\eta)$  for various values of Eckert number  $Ec$ ; ( $\xi, \beta = 0.2, M = 2, Pr = 1.0, \varepsilon = 0.1, \lambda = 1, m = 0.5$ )

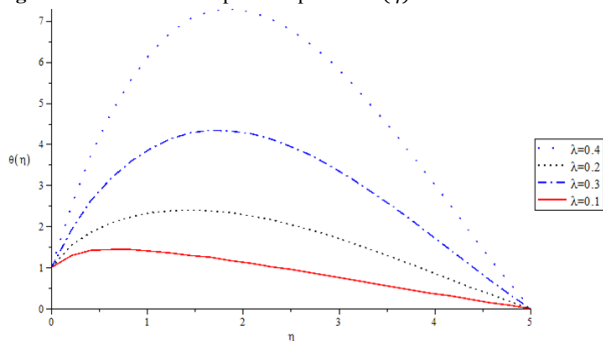
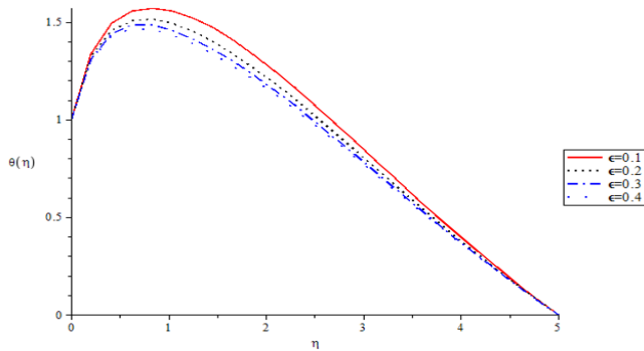
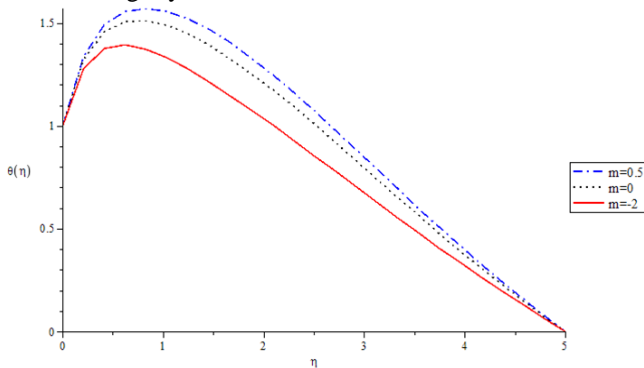


Fig. 10: Dimensionless temperature profiles  $\theta(\eta)$  for various values of Frank-Kameneskii parameter  $\lambda$ ; ( $\xi, \beta = 0.2, M = 2, Ec, Pr = 1.0, \varepsilon = 0.1, m = 0.5$ )



**Fig. 11:** Dimensionless temperature profiles  $\theta(\eta)$  for various values of Activation energy parameter  $\varepsilon$ ; ( $\xi, \beta = 0.2, M = 2, Ec, Pr = 1.0, \lambda = 0.1, m = 0.5$ )

**Fig.(12)** represents the dimensionless temperature profile  $\theta(0)$  for various values of chemical kinetics . It can be deduced that as  $m$  increases ( $-2,0,0.5$ ), the fluid temperature also increases reaching close to its maximum. Moreover, **Fig.(13)** represents the dimensionless entropy generation number ( $N_s$ ) for various values of the magnetic term  $M$ . It is shown that  $N_s$  increased slightly as  $M$  increases.



**Fig. 12:** Dimensionless temperature profiles  $\theta(\eta)$  for various values of Chemical kinetics parameter  $m$ ; ( $\xi, \beta = 0.2, M = 2, Ec, Pr = 1.0, \lambda, \varepsilon = 0.1$ )

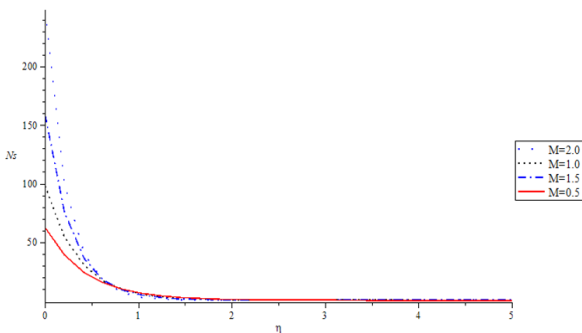


**Fig. 13:** Dimensionless entropy generation profiles  $N_s$  for various values of Magnetic parameter  $M$ ; ( $\xi, \beta = 0.2, Ec, Pr = 1.0, \lambda = 0.1, \varepsilon, m = 0.5$ )

**Fig.(14)** exhibits the variation of the dimensionless entropy generation number  $N_s$  for various values of  $\beta$ . It is pointed out that  $N_s$  is augmented as  $\beta$  increases. This is because increment in  $\beta$  causes higher velocity of the fluid particles and consequently increases the temperature. The variation of the dimensionless entropy generation number  $N_s$  for various values of  $\xi$  is demonstrated in **Fig.(15)**. It is observed that  $N_s$  decreases as  $\xi$  increases, this means that increase in the ratio of relaxation to retardation times retards  $N_s$ . **Fig. (16)** displays the variation of the dimensionless entropy generation number  $N_s$  against  $\eta$  for various values of  $\lambda$ . It is noticed that increase in  $\lambda$  causes  $N_s$  to increase and this is due to additional heat generated from the conversion of the kinetic energy of the fluid particle to heat energy, Frank-Kamenetskii parameter is one of the parameters to guide against energy loss. The variation of the dimensionless entropy generation  $N_s$  against  $\eta$  for various values of  $Re$  is depicted in **Fig. (17)**. It is noticed that increment in  $Re$  yields an increase in  $N_s$ . This is due to fluid friction and heat transfer inside the boundary layer.

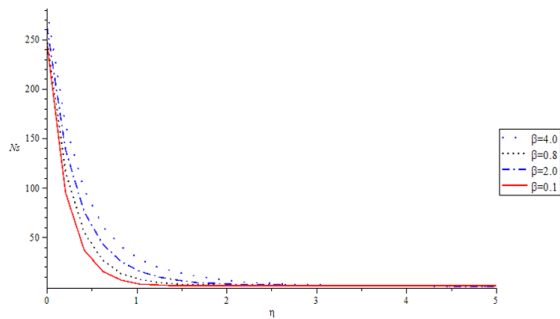


**Fig. 14:** Dimensionless entropy generation profiles  $N_s$  for various values of Deborah number  $\beta$ ; ( $\xi = 0.2, M = 2, Ec, Pr = 1.0, \lambda = 0.1, \varepsilon, m = 0.5$ )

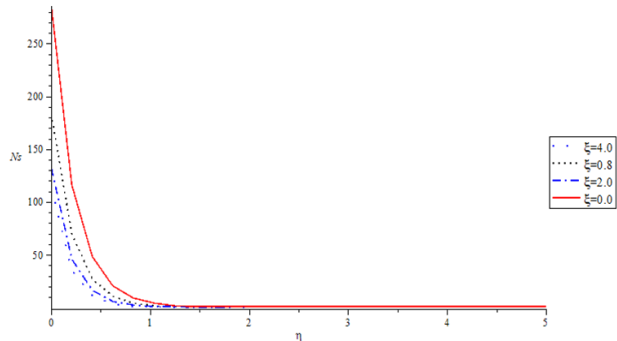


**Fig. 15:** Dimensionless entropy generation profiles  $N_s$  for various values of ratio of relaxation to retardation times  $\xi$ ; ( $\beta = 0.2, M = 2, Ec, Pr = 1.0, \lambda = 0.1, \varepsilon, m = 0.5$ )

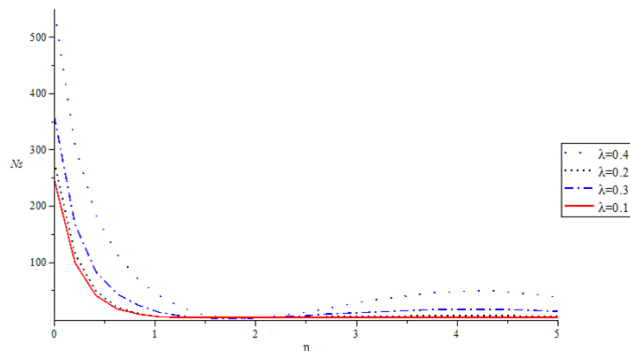


**Fig. 16:** Dimensionless entropy generation profiles  $N_s$  for various values of Frank-Kamenetskii parameter  $\lambda$ ; ( $\xi, \beta = 0.2, M = 2, Ec, Pr, \varepsilon = 1.0, m = 0.5$ )

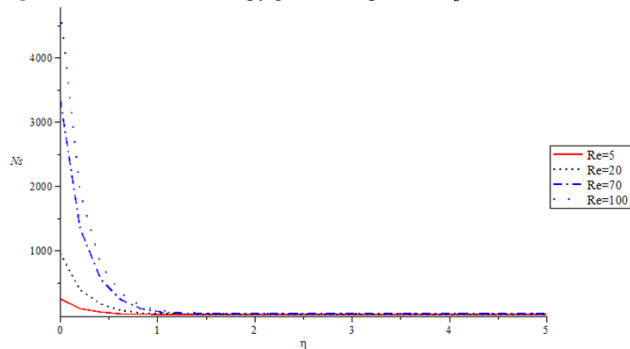


**Fig. 17:** Dimensionless entropy generation profiles  $N_s$  for various values of Reynolds number  $Re$ ; ( $\xi, \beta = 0.2, M = 2, Ec, Pr, \varepsilon = 1.0, \lambda = 0.1, m = 0.5$ )

**Fig.(18)** illustrates the impact of magnetic field term on dimensionless Bejan number profile ( $Be$ ) for the various magnetic term  $M$ . It is seen that magnetic term influences the Bejan number  $Be$  minimally at the boundary layer but increases rapidly as it moves away from the sheet.  $Be$  generally increases with an increase in  $M$ . **Fig.(19)** expresses the variation of the dimensionless Bejan number profile ( $Be$ ) against  $\eta$  for the various Deborah number  $\beta$ , it is seen that the Deborah number  $\beta$

decreases as Bejan number increases, the decrease became more noticeable or prominent at the distance away from the sheet. In Fig. (20), the dimensionless Bejan number profile ( $Be$ ) against  $\eta$  for the various ratio of relaxation to retardation times term  $\xi$  is depicted. It is seen that the ratio of relaxation to retardation times  $\xi$  has effect on  $Be$ , such that as  $\xi$  increases, the  $Be$  increases.

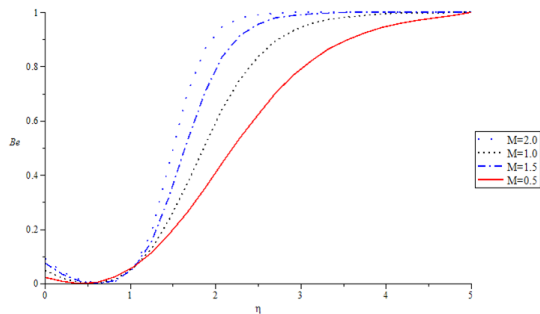


Fig. 18: Dimensionless Bejan profiles  $Be$  for various values of Magnetic parameter  $M$ ; ( $\xi, \beta = 0.2, Ec, Pr = 1.0, \lambda = 0.1, , m = 0.5$ )

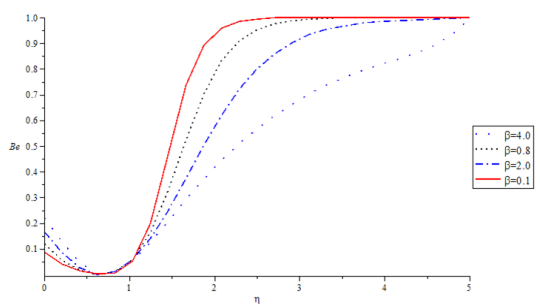


Fig. 19: Dimensionless Bejan profiles  $Be$  for various values of Deborah number  $\beta$ ; ( $\xi = 0.2, M = 2, Ec, Pr = 1.0, \lambda = 0.1, , m=0.5$ )

Fig. (21) highlights the dimensionless Bejan number profile ( $Be$ ) against  $\eta$  for the various Prandtl number  $Pr$ . It is seen that  $Pr$  generally boosts  $Be$  as it increases. While Fig.(22) displays the dimensionless Bejan number profile ( $Be$ ) for the various Eckerts number  $Ec$ . In particular, it is observed that  $Ec$  has effect on  $Be$ , it is seen that as  $Ec$  increases, so also does the Bejan profile.

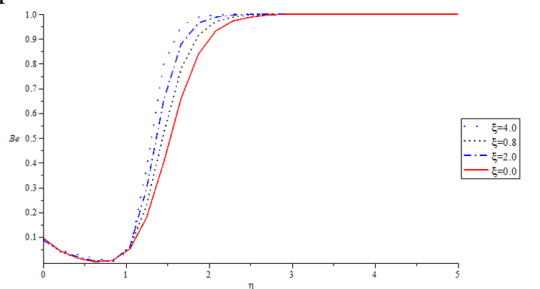


Fig. 20: Dimensionless Bejan profiles  $Be$  for various values of relaxation to retardation times  $\xi$ ; ( $\beta = 0.2, M = 2, Ec = 1.0, \lambda = 0.1, \varepsilon, m = 0.5$ )

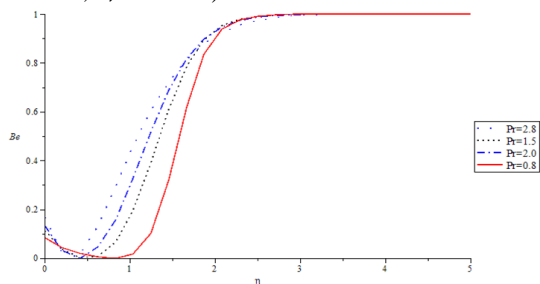
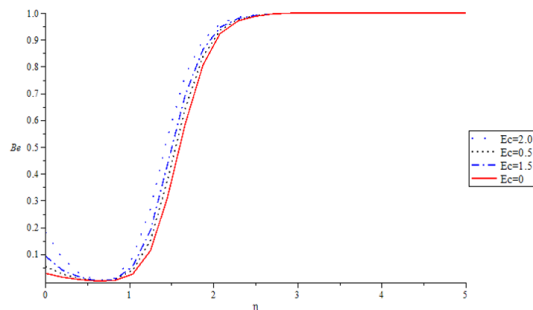
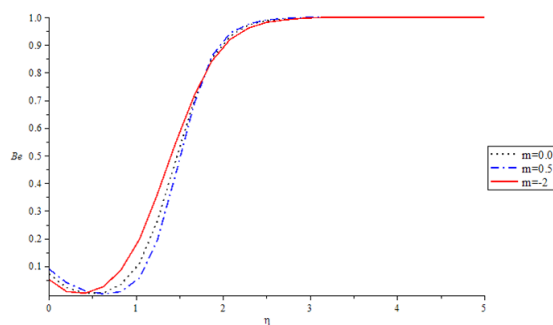


Fig. 21: Dimensionless Bejan profiles  $Be$  for various values of Prandtl number  $Pr$ ; ( $\xi, \beta = 0.2, M = 2, Ec = 1.0, \lambda = 0.1, \varepsilon, m = 0.5$ )

**Fig.(23)** indicates that chemical kinetics parameter reduces the Bejan number profile  $Be$  minimally as it moves from sensitized ( $m = -2$ ), to Arrhenius ( $m = 0$ ) and finally to Bimolecular ( $m = 0.5$ ) while **Fig.(24)** reveals that the Bejan Profile  $Be$  decreases near the sheet surface as  $Br$  increases.



**Fig. 22:** Dimensionless Bejan profiles  $Be$  for various values of Eckert number  $Ec$ ; ( $\xi, \beta = 0.2, M = 2, Pr = 1.0, \lambda = 0.1, m = 0.5$ )



**Fig. 23:** Dimensionless Bejan profiles  $Be$  for various values of Chemical kinetics parameter  $m$ ; ( $\xi, \beta = 0.2, M = 2, Ec, Pr, \varepsilon = 1.0, \lambda = 0.1$ )

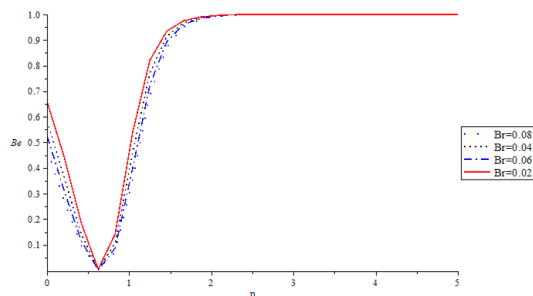


**Fig. 24:** Dimensionless Bejan profiles  $Be$  for various values of Brinkman number  $Br$ ; ( $\xi, \beta = 0.2, M = 2, Ec, Pr, \varepsilon = 1.0, \lambda = 0.1, m = 0.5$ )

## 5. Conclusion

The steady two dimensional flow of a reactive, magneto-hydrodynamic Jeffrey non-Newtonian incompressible fluid over a flat sheet, the sheet is assumed to be linear and isothermally stretching in nature. the numerical method; 4th Order Runge-Kutta based on shooting techniques was deployed after suitable similarity transformations were carried out on the momentum and energy equations. The effects of various flow and thermal parameter were considered and the results obtained are as follow:

- i. Increase in Ratio of relaxation to retardation times decreased both the dimensionless velocity profile and the dimensionless temperature profile.
- ii. Increase in Deborah number increased the dimensionless velocity profile and the dimensionless temperature profile.
- iii. Increase in Frank-Kameneskii parameter brought about magnanimous increase in dimensionless temperature profile, entropy generation profile and bejan profile due to its ability to contributed exothermic chemical reaction.
- iv. Increase in Magnetic term reduced the dimensionless velocity profile, increased the dimensionless temperature profile, has very little augmentation effect of entropy generation and significantly high effect on Bejan profile.

## References

- [1] B.C. Sakiadis, Boundary-layer behaviour on continuous solid surfaces: II. The boundary-layer on continuous flat surface. *AIChE J.* Vol. 7(1961), pp. 221-225, DOI: 10.1002/aic.690070211.
- [2] L. J. Crane, Flow past a stretching plate. *Z. Angew. Math. Phys.* 21(1970): 645-655.
- [3] M. M. Molla, and L. S. Yao, Mixed convection of non-Newtonian fluids along a heated vertical flat plate. *Int. J. Heat Mass Transfer* 52(2009): 3266-3271.
- [4] T. Hayat, R. Sajjad and S. Asghar, Series solution for MHD channel flow of a Jeffrey fluid. *Commun. Nonlinear Sci. Numer. Simul.* 15(2010): 2400-2406.
- [5] K. V. Prasad, P. S. Datti and K. Vajravelu, Hydrodynamic flow and heat transfer of a non-Newtonian power law fluid over a vertical stretching sheet. *Int. J. heat Mass Transfer* 53(2010): 879-888.
- [6] T. Hayat, Z. Iqbal, M. Mustafa and A. Alsaedi, Unsteady flow and heat transfer of Jeffrey fluid over a stretching sheet. (2012) <http://dx.doi.org/10.2298/TSCI110907092H>.
- [7] M. Qasim, Heat and mass transfer in a Jeffrey fluid over a stretching sheet with source/sink. *Alexandria Eng. J.* 52(2013) 571 – 575.
- [8] A. S. Idowu, K.M. Joseph and S. Daniel, Effect of Heat and Mass Transfer on Unsteady MHD Oscillatory Flow of Jeffrey Fluid in a Horizontal Channel with Chemical Reaction. *IOSR Journal of Mathematics*, Vol. 8(2013), Is. 5. pp: 74 - 87.
- [9] S. Nadeem, R. U. Haq and Z. H. Khan, Numerical solution of non-Newtonian nanofluid flow over a stretching sheet. *App. Nanosci.* 4(2014): 625-631.
- [10] A. S. Idowu, A. Jimoh and L. O. Ahmed, Impact of Heat and Mass Transfer on MHD Oscillatory Flow of Jeffrey Fluid in a Porous Channel with Thermal Conductivity, Dufour and Soret. *J. Appl. Sc. Environ. Manage.* Vol. 19(2015), No. 4, pp: 819 - 830.
- [11] S. Jena, S. R. Mishra, G. C. Dash, Chemical reaction effects on MHD Jeffrey fluid over a stretching sheet through porous media with heat generation/absorption. *Int. Jour. of App & Copm. Math.* Vol. 3(2)(2017): pp.1225 – 1238, doi:10.1007/S40819-016-0173-8.
- [12] L. Rundora, "Laminar flow in a channel filled with saturated porous media". *Ph. D. Thesis (2013), Cape Peninsula University of Technology*.
- [13] A. Bejan, Second Law Analysis in heat transfer. *Energy Int J.* 5(7) (1980): 21-23.
- [14] A. Bejan, Second Law Analysis in heat transfer and thermal design. *Adv. Heat Transf.* 15(1982): 1-58.
- [15] A. Bejan, Entropy generation minimization. Boca Raton, FL, New York, USA: CRC Pres; (1996).
- [16] A. S. Butt, S. Munawar, A. Ali and A. Mehmood, Entropy generation in hydrodynamic slip flow over a vertical plate with convective boundary *J. Mech. Sci. Technol.* 26 (9)(2012): 2977-2984
- [17] A.S. Butt and Ali, A. Entropy generation in MHD flow over a permeable stretching sheet embedded in a porous medium in the presence of viscous dissipation *Int. J. Exergy* 13 (2013) (1) 85-101
- [18] M. Dehsara, M. Habibi-Matin, N. Dalir, Entropy analysis for MHD flow over a non-linear stretching inclined transparent plate embedded in a porous medium due to solar radiation. *Mechanika* 18 (5) (2012): 524-533.
- [19] N. Dalir, Numerical study of entropy generation for forced convection flow and heat transfer of a Jeffrey fluid over a stretching sheet. *Alexandria Engineering Journal*(2014)53, 769 – 778, doi:10.1016/j.aej. 2014.08.005
- [20] S.O. Adesanya, S.O. Kareem, J.A. Falade, and S.A. Arekete, Entropy generation analysis for a reactive couple stress fluid flow through a channel saturated with porous material. *Energy* 93(2015): 1239 – 1245.
- [21] J. A. Gbadeyan, T. A.Yusuf, M. S. Dada, O. J. Akinremi, Effects Of slippage and couple stresses on entropy generation in a porous channel filled with highly porous medium. *Ilorin Journal of Science* 2(1) (2015): 48-67.
- [22] M. J. Uddin, O. A. Bég and A. I. Ismail, Radiative Convective Nanofluid flow past a stretching sheet with slip effects. DOI: 10.2514/1.T4372.
- [23] S. Das, A. S. Banu, R. N. Jana, O. D. Makinde, Entropy analysis on MHD pseudo-plastic nanofluid flow through a vertical porous with convective heating. *Ain Shams Eng. J.* 54(3)(2015): pp.325- 337, DOI: 10.1016/j.aej.2015.05.003.
- [24] B.J. Gireesha, B. Mahanthesh, P. T. Manjunatha, R. S. R. Gorla, Numerical solution for hydromagnetic boundary layer flow and heat transfer past a stretching surface embedded in non-Darcy porous medium with particle suspension. *Jour. of the nig. Math. Soc.* Vol. 34(3)(2015): pp.267 – 285, doi: 10.1016/j.jnms. 2015.07.003.
- [25] F. Mabood, R. G. Abdel-Rahman and Giulio Lorenzini, Numerical study of unsteady Jeffrey fluid flow with magnetic field effect and variable fluid properties. doi:10.115/1.4033013, *J. Thermal Sci. Eng. Appl.* 8 (4) (2016) 041003.
- [26] D. Cimpean, N. Lungu, I. Pop, A problem of entropy generation in a channel filled with a porous medium. *Creative Math. Int.* 17(2008):357-62

- [27] S. Paoletti, Rispoli F. and Sciubba E., Calculation of exergetic losses in compact heat exchanger passages, Tech. Rep. ASME, 10 (1989), 2, pp. 21 – 29.
- [28] S. Das and R. N. Jana, Entropy generation due to MHD flow in a channel with Navier slip. *Ain Shams Eng. J.* 5(2014): 575-584.
- [29] M. J. Uddin, O. A. Bég and N. Amin, Hydromagnetic Transport Phenomena from a Stretching or Shrinking Nonlinear Nanomaterial Sheet with Navier Slip and Convective Heating: A Model for Bio-Nano-Materials Processing, *Journal of Magnetism and Magnetic Materials*, Vol. 368,( 2014), pp. 252–261. doi:10.1016/j.jmmm.2014.05.041
- [30] A. Aziz, W. A. Khan, and I. Pop, Free Convection Boundary Layer Flow Past a Horizontal Flat Plate Embedded in Porous Medium Filled by Nanofluid Containing Gyrotactic Microorganisms, *International Journal of Thermal Sciences*, Vol. 56, (2012), pp. 48–57. doi:10.1016/j.ijthermalsci.2012.01.011
- [31] M. J. Uddin, M. Ferdows and O. A. Bég, Group Analysis and Numerical Computation of agneto-Convective Non-Newtonian Nanofluid Slip Flow from a Permeable Strtching Sheet, *Applied Nanoscience*, Vol. 4, No. 7, ( 2014), pp. 897–910.
- [32] A. Bachok, Ishak, and I. Pop, Stagnation Point Flow Toward a Stretching/Shrinking Sheet with a Convective Surface Boundary Condition, *Journal of the Franklin Institute*, Vol. 350, No. 9( 2013), pp. 2736–2744. doi:10.1016/j.jfranklin.2013.07.002
- [33] K. Autar, Runge-Kutta 4th Order for Ordinary Differential Equations. <http://numericalmethods.eng.usf.edu>
- [34] C.F. Gerald, and P.O. Wheatley, Applied numerical Analysis. 6th edition, Addison-Wesley Longman, (1999) USA.
- [35] D. B. Meade, B. S. Haran and R. E. White, The shooting technique for the solution of two-point boundary value problems. *Maple Tech.* 3 (1) (1996): pp.85-93.